HHS Public Access

Author manuscript

Nat Neurosci. Author manuscript; available in PMC 2015 February 01.

Published in final edited form as:

Nat Neurosci. 2014 August ; 17(8): 1083–1091. doi:10.1038/nn.3750.

Acid-sensing ion channels contribute to synaptic transmission and inhibit cocaine-evoked plasticity

Collin J. Kreple[1,2,*], **Yuan Lu**[3,*], **Rebecca J. Taugher**[4], **Andrea L. Schwager-Gutman**[9], **Jianyang Du**[5], **Madeliene Stump**[1,4], **Yimo Wang**[3], **Ali Ghobbeh**[3], **Rong Fan**[3], **Caitlin V. Cosme**[9], **Levi P. Sowers**[6], **Michael J. Welsh**[2,4,5,7,8], **Jason J. Radley**[4,9], **Ryan T. LaLumiere**[4,9], and **John A. Wemmie**[2,3,4,7,10]

[1]Medical Scientist Training Program, University of Iowa, Iowa City, Iowa, USA

[2]Department of Molecular Physiology and Biophysics, University of Iowa, Iowa City, Iowa, USA

[3]Department of Psychiatry, University of Iowa, Iowa City, Iowa, USA

[4]Interdisciplinary Graduate Program in Neuroscience, University of Iowa, Iowa City, Iowa, USA

[5]Department of Internal Medicine, University of Iowa, Iowa City, Iowa, USA

[6]Department of Neurology, University of Iowa, Iowa City, Iowa, USA

[7]Department of Neurosurgery, University of Iowa, Iowa City, Iowa, USA

[8]Howard Hughes Medical Institute, University of Iowa, Iowa City, Iowa, USA

[9]Department of Psychology, University of Iowa, Iowa City, Iowa, USA

[10]Department of Veterans Affairs Medical Center, Iowa City, Iowa, USA

Abstract

Acid-sensing ion channel 1A (ASIC1A) is abundant in the nucleus accumbens (NAc), a region known for its role in addiction. Because ASIC1A has been previously suggested to promote associative learning, we hypothesized that disrupting ASIC1A in the NAc would reduce drug-associated learning and memory. However, contrary to this hypothesis, we found that disrupting ASIC1A in the NAc increased cocaine-conditioned place preference, suggesting an unexpected role for ASIC1A in addiction-related behavior. Moreover, overexpressing ASIC1A in rat NAc reduced cocaine self-administration. Investigating the underlying mechanisms, we identified a novel postsynaptic current during neurotransmission mediated by ASIC1A and ASIC2 and thus well-positioned to regulate synapse structure and function. Consistent with this possibility, disrupting ASIC1A altered dendritic spine density and glutamate receptor function, and increased cocaine-evoked plasticity in AMPA-to-NMDA ratio, all resembling changes previously associated

Address Correspondence to: John A. Wemmie MD PhD, Roy J. and Lucille A. Carver College of Medicine, University of Iowa, Iowa City, IA 52242, Phone: 319-384-3173, Fax: 319-335-7623, john-wemmie@uiowa.edu.

*These authors contributed equally to this work

Author Contributions. All authors read and critiqued manuscript. CJK, YL, RJT, ALS, MS, YW, AG, RF, CVC, LPS, JJR performed experiments. CJK, YL, JD, MJW, JJR, LTL, JAW designed experiments. CJK, LY, RTL, JAW wrote manuscript. RTL and JAW provided funding for experiments.

with cocaine-induced behavior. Together, these data suggest ASIC1A inhibits plasticity underlying addiction-related behavior, and raise the possibility of therapies for drug addiction by targeting ASIC-dependent neurotransmission.

Keywords

ASIC1A; nucleus accumbens; cocaine; addiction

Introduction

Synapses in the nucleus accumbens (NAc) are altered by drugs of abuse. In NAc medium spiny neurons (MSNs) in rodents, cocaine exposure transforms dendritic spine density and morphology, alters glutamate receptor composition and function, and increases plasticity to subsequent cocaine exposure (for reviews see [1–3]). These synaptic responses are thought to underlie drug-related learning and memory, and increase incentive value of drugs and drug-seeking behavior. While numerous drug-related synaptic perturbations have been characterized in the NAc, much remains to be learned about the mechanisms that change these synapses and drive addiction.

Potential regulators of synapse physiology that are abundant in the NAc are Acid-Sensing Ion Channels (ASICs) [4]. ASICs are members of the Degenerin/Epithelial Na^+ Channel (DEG/ENaC) family that are formed by subunits in a trimeric structure and activated by low extracellular pH [5]. Different ASIC subunit combinations produce channels with different properties including pH sensitivity, ion selectivity, and pharmacological sensitivity [6,7]. Six ASIC subunits have been identified, although three (ASIC1A, ASIC2A, and ASIC2B) are most readily detectable in brain. Of these, ASIC1A is essential for currents evoked by acidosis in the physiological range (i.e. pH > 5) [4,7,8].

Accumulating evidence suggests that ASICs promote learning and memory. Loss of ASIC1A tended to reduce hippocampus-dependent learning in the Morris Water Maze [9], reduced cerebellum-dependent eye-blink conditioning [9], and reduced amygdala-dependent auditory cue and contextual fear conditioning [10]. Loss of ASIC1A also eliminated CO_2-potentiation of fear conditioning [11]. Whereas, transgenic over-expression of human ASIC1A in mice increased acid-evoked currents in brain neurons and enhanced fear conditioning [12].

Consistent with these behavioral studies, multiple observations indicate that ASIC1A and ASIC2 are present in the postsynaptic membrane and contribute to synaptic physiology. These proteins are relatively abundant at dendritic spines [9,12–14], enriched in synaptosome-containing brain fractions [9,12,14], and interact with the postsynaptic scaffolding proteins PSD-95 and PICK1 [14,15]. In mouse hippocampal slice cultures, extracellular acid increased Ca^{2+} entry into dendritic spines, an effect that depended largely on ASIC1A [13]. Perhaps as a consequence of this reduced Ca^{2+} entry, knocking down ASIC1A with siRNA decreased dendritic spine density in the hippocampus [13]. Furthermore, field excitatory post-synaptic potentials (fEPSPs) evoked during high-frequency stimulation were impaired in acute hippocampal slices from *Asic1a*$^{-/-}$ mice relative to wild-type controls, and a deficit in long-term potentiation (LTP) was detected [9], although the LTP deficit was not detected by

others [16]. Additionally, ASIC1A disruption increased mEPSC frequency and reduced paired-pulse ratios in microisland cultures of hippocampal neurons, suggesting that although ASIC1A has been detected in post-synaptic dendritic spines, it might also affect presynaptic release probability [17].

Despite these advances, significant gaps remain in our knowledge of ASICs in brain function and behavior. Importantly, the role of ASIC1A at synapses and its mechanism of activation remain unknown. One model posits that because synaptic vesicles are acidic, acidification of the synaptic cleft during neurotransmission might activate ASICs. However, to date no ASIC-dependent currents have been detected during synaptic transmission [9,16–18]. Likewise, while ASIC1A is abundantly expressed in the NAc [10], its role there is unknown. Here, we aimed to clarify the role of ASIC1A in the NAc by examining the effects of ASIC1A manipulation on addiction-related behavior, synaptic physiology, and morphology. Because previous studies suggest that ASIC1A promotes associative learning and synaptic plasticity, we hypothesized that ASIC1A would play a similar role in NAc-dependent learning and memory, and promote synaptic responses to drugs of abuse.

Results

ASIC1A in NAc affects drug-conditioned place preference

Because of the importance of the NAc in models of addiction and because previous studies suggest that ASIC1A promotes associative learning and memory, we hypothesized that disrupting ASIC1A would reduce addiction-related learning and memory. To test this hypothesis we used cocaine-conditioned place preference, which involves memory of a learned association between the rewarding effects of cocaine and an environmental context, is thought to model the ability of drug-associated environments to elicit craving and relapse, and depends on the NAc [19,20]. We started by testing *Asic1a*$^{-/-}$ mice. As with previous studies [10], we found that ASIC1A protein was relatively abundant in the NAc of wild-type mice but absent in *Asic1a*$^{-/-}$ mice (Fig. 1a). Similarly, extracellular application of acidic ACSF induced large currents from whole-cell recordings in NAc neurons in acute brain slices from wild-type mice, which were absent in *Asic1a*$^{-/-}$ mice (Fig. 1c). However, in contrast to our hypothesis, in conditioned place preference testing we found that *Asic1a*$^{-/-}$ mice spent a significantly greater amount of time in cocaine-paired contexts relative to wild-type mice (Fig. 1e). To test whether this effect of ASIC1A disruption was specific to cocaine or whether it generalized to multiple drugs of abuse, we also tested conditioned place preference to morphine, which is also known to depend on the NAc [21]. Like cocaine, conditioned place preference to morphine was also increased by ASIC1A disruption (Fig. 1f). This unexpected result raises the possibility that ASIC1A in the NAc might reduce drug-associated learning and memory.

To further determine whether the NAc is a key site of ASIC1A action in this behavior we utilized the Cre-Lox system. We found that injecting AAV-*Cre* into the NAc of *Asic1a*$^{loxP/loxP}$ mice bilaterally specifically reduced ASIC1A protein in the NAc detected by immunohistochemical staining (Fig. 1b) and western blot (Supplementary Fig. 2a). AAV-*Cre* also eliminated acid-evoked currents in virus-transduced NAc neurons (Fig. 1d, Supplementary Fig. 2b). Moreover, similar to whole-animal knockouts, *Asic1a*$^{loxP/loxP}$ mice

that received AAV-*Cre* in the NAc exhibited significantly greater cocaine-conditioned place preference compared with AAV-*eGFP*-injected controls (Fig. 1g).

Next, we tested whether expressing ASIC1A in the NAc could reverse the exaggerated cocaine-conditioned place preference observed in the *Asic1a*$^{-/-}$ mice. To express ASIC1A specifically in the NAc we bilaterally injected AAV-*Asic1a* [22]. We found that this virus induced ASIC1A-specific immunohistochemical staining in the NAc (Fig. 2a) and restored acid-evoked currents to normal levels in transduced neurons (Figs. 2b and 2c). Importantly, restoring ASIC1A in the NAc of *Asic1a*$^{-/-}$ mice with AAV-*Asic1a* reduced cocaine-conditioned place preference relative to AAV-*eGFP*-injected *Asic1a*$^{-/-}$ controls (Fig. 2d). In contrast, restoring ASIC1A in the dorsal hippocampus of *Asic1a*$^{-/-}$ mice did not alter cocaine-conditioned place preference (Supplementary Fig. 3). Because ASICs may mediate effects of global acidosis [11], we next tested whether cocaine grossly altered pH in the NAc with a fiberoptic pH sensor; unlike CO_2, cocaine (10 mg/kg, ip) produced no detectable pH change (Supplementary Fig. 4). Together these results suggest that ASIC1A plays a critical role in drug-related learning and memory, that the ASIC1A effects are reversible and not due solely to abnormal brain development, and that the NAc is a key site of ASIC1A action. Moreover, in contrast to its effects on other forms of learning and memory, these results suggest that ASIC1A in the NAc negatively regulates drug-associated learned place preference.

ASIC currents contribute to synaptic transmission in the NAc core

To better understand how ASIC1A may exert these unexpected behavioral effects we focused on synaptic transmission in the NAc. Synaptic vesicles are acidic and acidify the synaptic cleft [23–26]. Consequently, it has been speculated that protons released from neurotransmitter vesicles might activate ASICs at synapses [7,27,28]. Because ASIC1A is relatively abundant in the NAc, we reasoned that it might be possible to detect ASIC-dependent currents there during synaptic transmission, if they exist. To test this possibility, we measured evoked excitatory post-synaptic current (EPSC) in the NAc core by whole-cell voltage clamp in brain slices. We started with the ASIC-antagonist amiloride, which blocked a substantial portion of the EPSC which was independent of ASIC1A (Supplementary Fig. 5), consistent with its known effects on molecules other than ASICs [29,30]. However, after pharmacologically blocking AMPA, NMDA, and $GABA_A$ receptors, we found that amiloride inhibited a relatively small current that depended on ASIC1A (Fig. 3a). This current, detected in the postsynaptic cell, occurred in the same time frame as postsynaptic glutamate receptor activation, was nearly eliminated in the *Asic1a*$^{-/-}$ mice and was rescued to normal or slightly greater levels by restoring ASIC1A expression in the NAc with AAV-*Asic1a* (Fig. 3a, b). With changes in EPSC amplitude, the ASIC1A-dependent post-synaptic current remained a similar percentage of the total EPSC (Supplementary Fig. 6). Because ASIC2A has been suggested to help deliver ASIC1A to synapses through its interaction with PSD95 [14], we next tested whether the amiloride-sensitive postsynaptic current might be affected by manipulating ASIC2 subunits. Consistent with a role for ASIC2A or ASIC2B, we found that the amiloride sensitive postsynaptic current was significantly reduced in the *Asic2*$^{-/-}$ mice, in which both ASIC2 subunits are disrupted (Fig. 3c) [31]. We next tested the effects of psalmotoxin (PcTx1), which has been shown to inhibit ASIC1A homomeric

channels [32] and ASIC1A/ASIC2B heteromeric channels [33], but not ASIC1A/ASIC2A heteromeric channels [32]. PcTx1 had no effect on the amiloride-sensitive postsynaptic current in wild-type mice (Fig. 3c) and only partially inhibited the ASIC-mediated current evoked by extracellular acid (pH 5.6) (Fig. 3d). However, in the *Asic2*$^{-/-}$ mice, PcTx1 eliminated both the amiloride-sensitive postsynaptic current and the acid-evoked current (Fig. 3c, d). These results suggest that in the absence of ASIC2, the postsynaptic current is mediated by ASIC1A homomeric channels, and in the presence of ASIC2 the postsynaptic current is mediated by PcTx1-insensitive ASIC1A/ASIC2A heteromeric channels.

To assess the importance of pH dynamics in these these ASIC-dependent post-synaptic currents, we altered pH-buffering capacity of the extracellular solutions in slices by changing HCO_3 and CO_2 concentrations. Reducing the buffering capacity increased the ASIC-dependent post-synaptic current while increasing the buffering capacity reduced the ASIC-dependent current (Fig. 4a, b). Next, we tested whether the ASIC-dependent current is affected by carbonic anhydrase IV (CA-IV) an enzyme critical for regulating extracellular pH buffering in the brain [34]. We found that CA inhibition with acetazolamide and CA-IV disruption (*Car4*$^{-/-}$ mice) significantly increased the postsynaptic ASIC-dependent current (Fig. 4c, d), and that acetazolamide no longer exerted its effects in the absence of ASIC1A and CA-IV (Fig. 4c, e). Together these results suggest the existence of a novel postsynaptic current in the NAc that depends on ASIC1A and ASIC2, and is regulated by CA-IV and pH. By participating in the excitatory post-synaptic current in the NAc, ASIC1A may be well-positioned to influence plasticity and other aspects of synapse structure and function that may underlie the observed conditioned place preference behavior.

ASIC1A disruption increases dendritic spine density in NAc

Alterations in dendritic spine density and morphology in the NAc have been implicated in addiction-related behaviors [1]. This, coupled with previous data indicating that loss of ASIC1A reduces dendritic spine density in the hippocampus [13], led us to test whether ASIC1A disruption alters dendritic spine density and/or morphology in the NAc. To test this possibility, we filled MSNs in the NAc core with Lucifer yellow and quantified spine geometric features using *NeuronStudio* software. We found a significant increase in dendritic spine density in *Asic1a*$^{-/-}$ mice relative to *Asic1a*$^{+/+}$ mice (Fig. 5a, b). Analysis of spine subtypes revealed that the greater MSN spine densities in *Asic1a*$^{-/-}$ mice is largely attributable to a significant increase in stubby spines (Fig. 5c), and an upward trend of thin spine density (Fig. 5d), whereas mushroom spines were unaltered (Fig. 5e). These results suggest that ASIC1A influences either the formation or turnover of stubby and thin spines, which are thought to represent immature excitatory synapses [35]. Furthermore, these data indicate that ASIC1A disruption increases dendritic spine density in the NAc, which is in contrast to previously observed effects of ASIC1A in the hippocampus [13].

To determine whether this increase in spine density might lead to an increase in glutamatergic transmission, we assessed mEPSCs. We found that the frequency of mEPSCs was significantly increased in *Asic1a*$^{-/-}$ mice relative to *Asic1a*$^{+/+}$ controls (Fig. 5f, g, i), while mEPSC amplitude was unchanged (Supplementary Fig. 7). Likewise, restoring ASIC1A expression in the NAc with AAV-*Asic1a* normalized mEPSC frequency (Fig. 5f, h,

i). Because an increased mEPSC frequency might also be attributed to an increase in presynaptic release probability, we examined paired-pulse facilitation (PPF), a measure of release probability; we found no difference in PPF in the NAc between *Asic1a*$^{-/-}$ mice and their wild-type counterparts (Supplementary Fig. 8). Together, the increased density of dendritic spines accompanied by increased mEPSC frequency indicates that ASIC1A disruption increases the number of functioning excitatory synapses in the NAc, which resembles effects previously associated with increased cocaine-conditioned place preference [36].

Loss of ASIC1A alters glutamate receptor function in NAc

Accumulating evidence suggests that glutamate receptors in the NAc play a key role in addiction-related behavior [2,3]. More specifically, GluA2-lacking AMPA receptors, which are inward rectifying and Ca^{2+}-permeable, have been implicated in learning and memory and behavioral effects of cocaine, although their effects on cocaine-conditioned place preference have not yet been determined [37,38]. Thus, we tested whether loss of ASIC1A altered the AMPA receptor-rectification index. We found that AMPA receptors in the NAc of drug-naïve *Asic1a*$^{-/-}$ mice were significantly more inward rectifying than wild-type controls (Fig. 6a–c), suggesting an increase in GluA2-lacking AMPA receptors. Furthermore, we found that the rectification index, like cocaine-conditioned place preference, was normalized in the *Asic1a*$^{-/-}$ mice by virus-mediated ASIC1A expression in the NAc (Fig. 6a, b, d). These findings suggest that ASIC1A influences AMPA receptor composition at the synapse, which may contribute to cocaine-related learning and memory behavior.

Changes in the AMPA-to-NMDA ratio have also been implicated in cocaine-related learning and memory [38–40]. Therefore, we tested the effects of ASIC1A on the AMPA-to-NMDA ratio. Drug-naïve *Asic1a*$^{-/-}$ mice exhibited an increase in the AMPA-to-NMDA ratio relative to drug-naïve *Asic1a*$^{+/+}$ mice (Fig. 7a, b). In addition, as with conditioned place preference and AMPA receptor-rectification, restoring ASIC1A expression to the NAc with AAV-*Asic1a* normalized the AMPA-to-NMDA ratio (Fig. 7a, b), indicating that these effects of ASIC1A disruption are plastic and reversible. While an increase in AMPA-to-NMDA ratio in the *Asic1a*$^{-/-}$ mice may seem inconsistent with a lack of change in mEPSC amplitude, the same combination of effects in the NAc core has been previously associated with cocaine-related synaptic plasticity [40]. The effect is thought to be due to an increase in synaptic AMPA receptors [40], though a reduction in NMDA receptors remains possible.

Loss of ASIC1A increases cocaine-evoked plasticity

Previous studies by others suggest that following withdrawal from repeated cocaine administrations, the AMPA-to-NMDA ratio in the NAc of wild-type mice is sensitive to a single cocaine dose, whereas the AMPA-to-NMDA ratio in drug-naïve mice is unaffected [39]. Because the synaptic changes observed above in the *Asic1a*$^{-/-}$ mice resembled changes following withdrawal, we hypothesized that the AMPA-to-NMDA ratio in drug-naïve *Asic1a*$^{-/-}$ mice may be sensitive to a single cocaine challenge. To test this hypothesis, we measured the effects of a single cocaine dose (10 mg/kg, ip) on the AMPA-to-NMDA ratio in the NAc of drug-naïve wild-types and *Asic1a*$^{-/-}$ mice. We found that a

single dose of cocaine reduced the AMPA-to-NMDA ratio in drug-naïve *Asic1a*$^{-/-}$ mice 24 hours after administration (Fig. 7c, d). In contrast, the single cocaine challenge did not alter the AMPA-to-NMDA ratio in wild-type mice unless they had been previously withdrawn from cocaine (Fig. 7c, d). Interestingly, in cocaine-withdrawn *Asic1a*$^{-/-}$ mice the AMPA-to-NMDA ratio was lower than drug-naïve *Asic1a*$^{-/-}$ mice and was unaffected by a subsequent cocaine challenge. Of note, as indicated in the literature [39], single and repeated saline injections alone did not affect the AMPA-to-NMDA ratio in *Asic1a*$^{+/+}$ or *Asic1a*$^{-/-}$ mice (Fig. 7d, e). These results suggest that relative to wild-type mice, ASIC1A disruption alters cocaine-evoked plasticity at glutamatergic synapses in the NAc.

ASIC1A attenuates cocaine self-administration in rats

The results above suggest that ASIC1A opposes cocaine-related learning and memory, and cocaine-related synaptic changes. Therefore we hypothesized that enhancing ASIC1A function might reduce cocaine-taking behavior, which is most tractably tested by operant drug self-administration behavior in rats. We found that injecting AAV-*Asic1a* into the NAc of rats increased ASIC1A protein in the NAc detected by western blot (Fig. 8a), and increased acid-evoked current in virus-transduced MSNs (Fig. 8b, c). Importantly, in rats, as in mice, we identified an ASIC1A-dependent post-synaptic current; this current was doubled by ASIC1A overexpression (Fig. 8d). Moreover, three-weeks post-virus transduction, overexpressing ASIC1A in the NAc produced a rightward shift in the cocaine dose-response curve and reduced the total number of self-administered infusions (Fig. 8e). These findings suggest that overexpressing ASIC1A in the NAc reduces the reinforcing properties of cocaine.

Discussion

The above results suggest that ASIC1A plays a critical role in the NAc. We found that ASIC1A disruption increased cocaine-evoked plasticity in the NAc and increased cocaine-conditioned place preference, a model of drug reward-associated learning and memory [19,20]. Although cocaine-conditioned place preference does not specifically distinguish between effects on reward versus learning or memory, these results were unexpected because they were in apparent contrast with the previously observed effects of ASIC1A in promoting learning and memory in amygdala-, cerebellum-, and hippocampus-dependent behaviors [7,10–12,22], synaptic plasticity [7,13], and dendritic spine density [13]. While ASIC1A may promote some forms of learning, memory, and plasticity, the results described here suggest that ASIC1A may also inhibit others. The finding that ASIC1A overexpression in the rat NAc reduces self-administration suggests that ASIC1a affects the reinforcing properties of cocaine, which likely play a critical role in cocaine conditioned place preference. Together these outcomes suggest that the behavioral impact of ASIC1A function may differ depending on brain site, specific circuit, or behavioral task. Although this observation is novel for ASICs, opposite actions of molecules in the NAc versus other brain regions is not unprecedented; BDNF also appears to produce opposite effects in the NAc versus the hippocampus in depression-related phenotypes [41,42]. Our results raise the need to better understand the action of ASICs in other brain areas and how this action influences other forms of learning, memory, and behavior. Nevertheless, our analyses of synaptic

function and structure outlined here begin to suggest how ASIC1A may reduce NAc-dependent cocaine-related behavior.

The identification of an ASIC-dependent current during synaptic transmission is novel and is likely critical for the behavioral effects observed here. The small size of this postsynaptic current relative to glutamate receptor-mediated current may help explain why it has previously eluded detection. Several observations suggest that this postsynaptic current is ASIC-mediated. First, ASIC1A is present at dendritic spines [7,13,14]. Second, the current was completely inhibited by the pan-ASIC blocker amiloride. Third, disrupting ASIC1A nearly eliminated the current. Fourth, disrupting ASIC2 attenuated the current. Finally, in *Asic2*$^{-/-}$ mice, PcTx1 completely eliminated the current. In addition, we tested the effects of pH-buffering capacity and the critical pH-buffering enzyme in the brain, CA-IV [34]. The ability of acetazolamide and/or genetically disrupting CA-IV to increase the ASIC-dependent postsynaptic current strongly suggests a role for pH in its activation. Because during synaptic transmission the most likely source of protons is from presynaptic neurotransmitter-containing vesicles [23,25,26,43], detecting an ASIC-dependent component of the EPSC strengthens previous assertions that protons may act as neurotransmitters [44]. By contributing to neurotransmission, these results suggest ASICs are well-positioned to alter membrane voltage and synaptic [Ca^{2+}], which could increase or decrease synaptic strength depending on timing and magnitude, and could produce diverse effects on synapse structure and function [4,45,46]. ASIC interactions with other proteins including PICK1, PSD95, NMDA receptors, and voltage-gated Ca^{2+} channels might also be involved [4,45,46].

Importantly, the synaptic changes induced in the NAc by loss of ASIC1A were strikingly similar to synaptic adaptations observed previously by others in mice and rats following cocaine withdrawal, and thought to underlie increased cocaine-associated behaviors other than cocaine-conditioned place preference [37–40]. The mechanisms by which cocaine induces these synaptic changes is not fully understood; thus it remains difficult to discern if and how the ASIC1A-related changes might intersect with those evoked by cocaine. Paralleling these previously observed effects of cocaine withdrawal on synapses in the NAc, we found that ASIC1A disruption increased AMPA-to-NMDA ratio, AMPA receptor rectification index, mEPSC frequency, and density of stubby dendritic spines. Several studies have reported altered spine density and morphology in the NAc following cocaine withdrawal [47]. Interestingly, the most obvious morphological effect observed following ASIC1A disruption was an increase in stubby spines, a spine type that to our knowledge has not been implicated in cocaine-dependent effects. The precise function of stubby spines remains poorly understood, although they are most abundant during development and are thought to be immature and highly plastic (for review, see [48]). The increase in total spine density in MSNs of *Asic1a*$^{-/-}$ mice is consistent with the increased mEPSC frequency. Previous studies have also associated an increased mEPSC frequency with increased stubby spine density in the NAc [49]. Taken together these results suggest that ASIC1A may help establish or maintain synapse maturity in the NAc. The reversibility of at least some of these changes in adult mice by viral vectors driving ASIC1A expression supports a post-developmental role for ASIC1A. Perhaps most relevant to the increased cocaine-dependent behavior in the *Asic1a*$^{-/-}$ mice was the finding that a single dose of cocaine altered the AMPA-to-NMDA

ratio in *Asic1a*$^{-/-}$ mice, but not in their wild-type counterparts, suggesting that cocaine-evoked synaptic plasticity is exaggerated in the *Asic1a*$^{-/-}$ mice.

The observation that ASIC1A disruption increased morphine-conditioned place preference as well as cocaine-conditioned place preference, suggests that the behavioral effects of ASIC1A may generalize to multiple drugs of abuse and to other models of drug-related behavior. Consistent with this possibility, a recent study suggests that ASIC1A disruption decreased the acute locomotor response to cocaine [50]. Because the NAc has been implicated in other appetitive behaviors, including food consumption, it would be interesting to know whether ASIC1A alters such appetitive drives. Although *Asic1a*$^{-/-}$ mice do not normally differ in weight from wild-type mice when fed ad libitum (Supplementary Fig. 9), they consumed more sucrose following chronic mild stress, suggesting a possible role for ASIC1A in stress-evoked appetitive behaviors that depend on the NAc [22]. Recent studies have focused on the contrasting roles of D1 and D2 neurons in the NAc. While more work is needed to determine which of these cell types might be important for the behavioral effects of ASIC1A observed here, we speculate that ASIC1A functions in both cell populations because our electrophysiological recordings likely sampled both D1 and D2 neurons, and all of the wild-type MSNs tested here had ASIC-like currents.

Together, the data and observations presented here suggest a model whereby ASICs contribute to synaptic transmission in the nucleus accumbens, which alters synaptic structure and function likely through postsynaptic depolarization and/or increased $[Ca^{2+}]_c$, and consequently reduces cocaine-evoked plasticity and cocaine-related behavior. These findings raise the exciting possibility that ASIC1A in the NAc may reduce vulnerability to addiction, and suggest novel therapeutic avenues targeting pH, carbonic anhydrase, or ASICs at the synapse.

Methods

Mice

All mice tested were maintained on a C57BL/6 genetic background. These mouse strains tested include wild-type C57BL/6, *Asic1a*$^{-/-}$, *Asic2*$^{-/-}$, *Car4*$^{-/-}$ and *Asic1a*$^{loxP/loxP}$. *Asic1a*$^{-/-}$ and *Asic2*$^{-/-}$ mice were described previously [9,31] as were *Car4*$^{-/-}$ mice [34]. *Asic1a*$^{loxP/+}$ mice were obtained from Xenogen Biosciences and intercrossed to produce the *Asic1a*$^{loxP/loxP}$ strain. The strategy for developing these mice is illustrated (Supplementary Fig. 1). Briefly, exon 2 was selected as the conditional knockout region. The targeting vector contained a neomycin resistance cassette, which was removed at the embryonic stem cell stage by flippase transfection. All mice were housed in groups of 2–5, kept on a standard 12 hour light-dark cycle, and fed standard chow and water ad libitum. All experiments were performed during the light cycle. All experimental groups were matched for age (10–15 weeks) and sex. Mice in a given housing group were randomly assigned to a treatment group such that each housing group contained animals with different treatments (e.g. for injection of AAVs, each housing group contained a mouse treated with AAV-*Asic1a* and AAV-*eGFP*). All mice used were naïve to any experimentation at the beginning each experiment performed. Animal care met National Institutes of Health standards, and the University of Iowa Animal Care and Use Committee approved all experiments.

Conditioned Place Preference

A two-sided chamber was used: one side with black walls and rod floors, and the other side with white walls and mesh floors. A 5-day protocol was utilized. Day 1 consisted of a 20-minute pre-test period in which animals were allowed to explore both chamber sides. Mice spending more than 75% time in either side were excluded. Days 2–4 involved two training periods (one in the morning and one in the afternoon) in which animals were injected with cocaine (10 mg/kg, diluted in 0.9% saline, i.p., 10 μl/g body mass, Sigma Aldrich) or 0.9% saline alone (10 μl/g body mass) and confined to one side of the chamber for 30 minutes. The context paired with cocaine was counterbalanced for all experiments. Conditioned place preference was determined on day 5; a blinded observer quantified time spent on the side previously paired with cocaine during a 20-minute choice period. Place preference was determined by subtracting the time spent in the cocaine-paired context on day 1 (pre-test) from time spent in the cocaine-paired context on day 5 (test). Morphine conditioned place preference was assessed with the same protocol, except after the day-1 pre-test mice received a single injection per day for 6 days: saline (0.9%, 10 μl/g body mass, i.p.) was administered on days 2, 4, and 6, and morphine (10 mg/kg in 0.9% saline, i.p.) on days 3, 5, and 7 and subsequently confined to one side of the chamber for 40 minutes.

Virus Injections

Viral vectors were produced by the University of Iowa Gene Transfer Vector Core and were injected bilaterally as described previously [22]. Viral vectors were adeno-associated viruses (AAV) 2/1, with AAV1 capsids and AAV2 ITRs. A CMV promoter was used to drive ASIC1A, eGFP, or Cre expression. AAV-*eGFP* was co-injected with all AAV-*Asic1a* and AAV-*Cre* injections as described previously [22]. Nucleus accumbens coordinates utilized were as follows (relative to bregma): anteroposterior +1.2 mm, lateral 1 mm, ventral 3.9 mm from pial surface. Dorsal hippocampus coordinates utilized were as follows (relative to bregma): anteroposterior −1.5 mm, lateral 1 mm, ventral 1.5 mm from pial surface. Mice were allowed to recover 21–28 days following the injection. Targeting was confirmed post-mortem as previously described [22]. Hits were defined by fluorescence above background in the nucleus accumbens bilaterally.

NAc Slice Physiology

Coronal NAc brain slices (300 μm) were prepared from 8–12 week old male mice. Briefly, NAc slices were cut using a Vibratome 1000 Plus (Vibratome, St. Louis, MO) in ice-cold slicing buffer (in mM: 127 NaCl, 26 $NaHCO_3$, 1.2 KH_2PO_4, 1.9 KCl, 1.1 $CaCl_2$, 2 $MgSO_4$, 10 D-Glucose) bubbled with 95% O_2 and 5% CO_2. Slices were then transferred to a holding chamber containing oxygenated artificial cerebrospinal fluid (ACSF; in mM: 127 NaCl, 26 $NaHCO_3$, 1.2 KH_2PO_4, 1.9 KCl, 2.2 $CaCl_2$, 1 $MgSO_4$, 10 D-Glucose) for 30 min at 34°C and for another 30 min at 22°C for recovery, and then transferred to a submersion recording chamber continually perfused with 32°C oxygenated ACSF (rate: 2 ml/min). Slices were equilibrated for at least 15 min before each recording.

Electrophysiology

Whole-cell recordings from NAc core neurons were made by experimenter blinded to genotype and treatment group using an Axopatch 200B amplifier (Axon Instruments, Foster City, CA), sampled at 10 kHz, digitized by a DigiData 1322A, and later analyzed off-line by ClampFit (Axon software). NAc medium spiny neurons (MSNs) were identified under DIC microscopy (Nikon Eclipse E600FN) by their morphology. Recording pipettes with resistances ranging between 3–6 MΩ were pulled using standard borosilicate capillaries by a Flaming-Brown electrode puller (P-97, Sutter Instruments Co., Novato, CA) and were filled with a Cs-methanesulfonate based patch solution (in mM: 125 Cs- methanesulfonate, 20 CsCl, 10 NaCl, 2 Mg-ATP, 0.3 Na-GTP, 2.5 QX314, 10 HEPES, 0.2 EGTA, pH 7.3 adjusted with CsOH) for experiments measuring AMPAR rectification and AMPAR-to-NMDAR ratio. For AMPAR rectification, 100 μM spermine added to the patch pipette solution. K-gluconate based patch solution (in mM: 125 K-Gluconate, 20 KCl, 10 NaCl, 2 Mg-ATP, 0.3 Na-GTP, 2.5 QX314, 10 HEPES, 0.2 EGTA, pH 7.3 adjusted with KOH) was used for all the other whole-cell recordings. EPSCs were evoked with a bipolar tungsten electrode. To determine AMPAR-to-NMDAR ratio, peak amplitude of ESPCs at −70 mV in presence of 100 μM picrotoxin, was measured as AMPAR-mediated currents and peak amplitude of EPSCs at +50 mV, in presence of 100 μM picrotoxin and 20 μM CNQX, was measured as NMDAR-mediated currents. To determine AMPAR rectification, the peak amplitude of ESPCs, in presence of 100 μM picrotoxin and 100 μM DL-APV, was measured as AMPAR-mediated currents ranging from −70 mV to +70 mV in 20 mV steps. Liquid junction potential was uncompensated, and EPSC reversal was consistently around +10 mV. Rectification index was measured as the ratio between peak amplitude of EPSCs at −70mV and +50 mV. AMPAR-mediated miniature EPSCs (mEPSCs) were recorded from NAc core neurons with a holding potential at −70 mV, in presence of 1 μM tetrodotoxin (TTX, Tocris) and 100 μM picrotoxin. 1 μM TTX was used to block voltage-gated Na^+ channels, 20 μM CNQX was used to block AMPA receptors, 100 μM picrotoxin was used to block $GABA_A$ receptors, and 100 μM DL-APV was used to block NMDA receptors. In addition, 200 and 500 μM acetazolamide were used to block carbonic anhydrase, 500 μM amiloride or 100 nM psalmotoxin 1 (PcTx1) was used to block ASICs. To test electrophysiological effects of cocaine withdrawal, cocaine (10 mg/kg in 0.9% saline, i.p.) was injected once per day for 7 days, and for the following 7 days animals were withdrawn from cocaine. A challenge dose of cocaine (10 mg/kg in 0.9% saline, i.p.) or saline was given on day 7 of withdrawal. To confirm that repeated saline injections and the associated pain and stress did not alter the AMPA-to-NMDA ratio, in a separate experiment we modeled the cocaine injection protocol but instead injected saline repeatedly for 7 days, followed by 7 days of no injections in home cage, followed by a single saline injection. Brains slices were obtained 24 hours later for electrophysiological analysis. To test effects of a single dose of cocaine, animals were injected with either cocaine (10 mg/kg in 0.9% saline, i.p.) or saline and 24 hours later brain slices were obtained for electrophysiological analysis.

Intracellular dye injections and spine morphologic analyses

The procedures employed for the assessment of dendritic spine density and morphology in the NAc were based upon a previous report [51]. Briefly, drug naïve wild type and *Asic1a*$^{-/-}$

mice were anesthetized using ketamine/xylazine and transcardially perfused using 1% paraformaldehyde in PBS, followed by perfusion with 4% paraformaldehyde/0.125% glutaraldehyde in PBS. 250 μm-thick coronal sections containing the NAc were then obtained, and NAc core MSNs were identified by their morphology and injected with 5% Lucifer yellow (Invitrogen) via iontophoresis through micropipettes (1–2 μm inner diameter) under a direct current of 1–6 nA for 5 minutes. Sections were then mounted onto glass slides and coverslipped in VectaShield (Vector Laboratories). All imaging of dendritic segments was performed using a Leica SP5 confocal microscope with a 100X, 1.4 N.A. oil-immersion objective, using voxel dimensions of 0.1 × 0.1 × 0.1 μm^3. Non-overlapping, completely filled dendritic segments from the NAc core were randomly selected at a distance between 50–150 μm from the soma for high-resolution imaging. Images were deconvolved with AutoDeblur (Media Cybernetics), and 3D analyses were performed using the semi-automated software *NeuronStudio* to characterize spine density and morphometric features (i.e., head/neck diameter, length) for each dendritic spine [52,53] (http://research.mssm.edu/cnic/tools-ns.html). *NeuronStudio* also classifies dendritic spines into categories (thin, mushroom, stubby) based upon user-defined parameters: thin or mushroom spines were designated if the head-to-neck diameter ratio was >1.1: 1. Within this subdivision, spines with a head diameter >0.35 μm were classified as mushroom, or otherwise classified as thin. Spines with head-to-neck diameter ratios <1.1: 1 were also classified as thin if the ratio of spine length-to-neck diameter was greater than 2.5, otherwise they were classified as stubby. Filopodial spines, having a long and thin shape with no enlargement at the distal tip, were very seldom observed and classified herein as thin. An average of 4 neurons was imaged per mouse. 2–4 dendritic segments were imaged per neuron. 6227 dendritic spines were analyzed in total (3032 spines in *Asic1a*$^{+/+}$ mice, 3195 spines in *Asic1a*$^{-/-}$ mice).

NAc dissection and Western blotting

The NAc was dissected from the brain using a mouse brain matrix (Kent Scientific) and tissue punches (Harris Uni-core). Dissected tissue was then homogenized in cold 1% Triton X-100 lysis buffer phosphate-buffered saline (PBS) and protease inhibitors (Roche Complete, Mini). Protein concentration was determined using the BCA assay (Pierce Protein Research Products). 7.5 μg was run on 4–12% Bis-Tris gel (Invitrogen NuPAGE Novex Tris-Acetate Mini Gel) and transferred to a PVDF membrane for Western blotting (Immobilon-FL, Millipore). The membrane was blocked for 1 hour at room temperature with a blocking buffer of 0.1% casein, 0.01% sodium azide in tris-buffered saline containing 0.5% Tween (TBS-T). The membrane was then incubated for 2 hours at room temperature with primary antibodies in blocking buffer, and washed three times with TBS-T. Primary antibodies were used as follows: rabbit polyclonal anti-ASIC1 antiserum (MTY19 [10]) diluted 1:500 and chicken polyclonal anti-GAPDH antibody (Millipore AB2302) diluted 1:10000. The membrane was incubated for 1 hour at room temperature with secondary antibodies diluted in blocking buffer with 0.15% SDS, washed three times with TBS-T and washed three times with PBS. Secondary antibodies used were IRDye 800CW Donkey anti-Rabbit IgG and IRDye 680LT Donkey anti-Chicken IgG (LI-COR, 926-68028) (1:10000). Membranes were imaged using the odyssey imaging system (LI-COR). Western blotting results were repeated at least twice with no limitations in reproducibility.

Immunohistochemistry

Coronal slices (12 μm) of fresh frozen brain were produced and mounted on slides using the CryoJane sectioning system (Electron Microscopy Sciences). Slides were then postfixed in PBS with 4% paraformaldehyde and 4% sucrose for 10 minutes, followed by 0.25% Triton X-100 in PBS for 5 minutes at room temperature. This was followed by incubation in rabbit polyclonal anti-ASIC1 antiserum (MTY19 [10]) (1:1000) for 24 hours at 4°C. The slides were then washed in PBS and subsequently incubated in Alexa Fluor 568-coupled anti-rabbit IgG (Invitrogen, A-11011) (1:500) for 1 hour at room temperature. Slices were visualized using a Zeiss confocal microscope (Zeiss 710). Images were compiled at 10x magnification and compiled using the Zeiss tiling function. Immunohistochemical results were repeated at least twice with no limitations in reproducibility.

Measuring Brain pH during cocaine injection and CO_2 inhalation

A fiber optic pH sensor (pHOptica, WPI, detection range pH 5–9) was placed in the NAc (relative to bregma: anteroposterior +1.2 mm, lateral 1 mm, ventral 3.9 mm from pial surface) in a wild-type mouse anesthetized with ketamine/xylazine. Brain pH was measured in response to 20% CO_2 inhalation (21% O_2, N_2 balanced) or cocaine (10 mg/kg in 0.9% saline, i.p.).

Rat self-administration and virus injections

ASIC1A was overexpressed by injecting 0.5 μl of AAV2/1-CMV- *Asic1a (mouse)* or AAV2/1-CMV-eGFP bilaterally into the NAc of male Sprague-Dawley rats at a rate of 0.1 μl/min. Coordinates were as follows: anteroposterior +1.7 mm, lateral 1.6 mm, ventral 7.5 mm, relative to skull surface. Control rats received AAV2/1-CMV-*eGFP* alone. Two weeks later, intra-jugular venous catheters were implanted. Rats recovered for 1 week before beginning training on cocaine self-administration using previously described procedures [54]. Briefly, self-administration procedures were carried out in operant boxes equipped with two levers (Med Associates, Fairfield, VT). During daily 2-hour sessions, rats were trained to press a lever on an FR1 schedule of reinforcement to receive 50 μl infusions of cocaine (300 μg/infusion; cocaine dissolved in 0.9% sterile saline; cocaine-HCI kindly provided by NIDA). Criteria to begin the dose-response study were at least five days of self-administration, including at least 15 infusions per session on the last two days. After reaching these criteria, rats underwent one day of self-administration with each cocaine dose, in descending order (300, 90, 30, 9, 3 μg/infusion).

Statistical Analysis

All bar graphs express values as mean ± standard error of the mean (SEM). Distribution normality was assessed with the D'Agostino-Pearson omnibus test. Student's t-test was used to determine significance between two groups and Welch's correction was used when indicated by F-test for equality of variance. One-way analysis of variance (ANOVA) was used to assess differences between more than two groups. When variances differed significantly as measured by Bartlett's test, a Kruskal-Wallis one-way ANOVA (with Dunn's post-hoc tests) was used. Two-way ANOVA was used to test for interactions between two independent variables. Sample sizes were estimated *a priori* from previously

detected large effects of disrupting *Asic1a* and other genes, where similar sample sizes typically have been sufficient to achieve $\alpha < 0.05$ and power > 0.80. P values (two-tailed, unless otherwise noted) less than 0.05 were considered significant. Graphpad Prism was utilized for all statistical analyses. A supplementary methods checklist is available.

Supplementary Material

Refer to Web version on PubMed Central for supplementary material.

Acknowledgments

We thank Michael Lutter and Margaret Price for critically reading the manuscript. We also thank Margaret Price for providing *Asic2*$^{-/-}$ mice. We thank the University of Iowa Gene Transfer Vector Core and Central Microscopy Research Facility. J.A.W. was supported by the Department of Veterans Affairs (Merit Award), the NIMH (5R01MH085724), the NHLBI (R01HL113863) and a NARSAD Independent Investigator Award. J.J.R. was supported by the National Institutes of Health (MH095972). R.T.L. was supported by the National Institutes of Health (DA034684). C.J.K was supported by the University of Iowa Interdisciplinary Training Program in Pain Research NINDS T32NS045549. M.J.W. is an Investigator of the Howard Hughes Medical Institute.

References

1. Russo SJ, et al. The addicted synapse: mechanisms of synaptic and structural plasticity in nucleus accumbens. Trends Neurosci. 2010; 33:267–276. S0166-2236(10)00020-2 [pii]. 10.1016/j.tins.2010.02.002 [PubMed: 20207024]
2. Luscher C, Malenka RC. Drug-evoked synaptic plasticity in addiction: from molecular changes to circuit remodeling. Neuron. 2011; 69:650–663. S0896-6273(11)00065-1 [pii]. 10.1016/j.neuron.2011.01.017 [PubMed: 21338877]
3. Kalivas PW. The glutamate homeostasis hypothesis of addiction. Nat Rev Neurosci. 2009; 10:561–572.10.1038/nrn2515 [PubMed: 19571793]
4. Wemmie JA, Taugher RJ, Kreple CJ. Acid-sensing ion channels in pain and disease. Nat Rev Neurosci. 2013; 14:461–471. nrn3529 [pii]. 10.1038/nrn3529 [PubMed: 23783197]
5. Jasti J, Furukawa H, Gonzales EB, Gouaux E. Structure of acid-sensing ion channel 1 at 1.9 A resolution and low pH. Nature. 2007; 449:316–323. nature06163 [pii]. 10.1038/nature06163 [PubMed: 17882215]
6. Hesselager M, Timmermann DB, Ahring PK. pH-dependency and desensitization kinetics of heterologously expressed combinations of ASIC subunits. J Biol Chem. 2004; 279:11006–11015. [PubMed: 14701823]
7. Benson CJ, et al. Heteromultimerics of DEG/ENaC subunits form H^+-gated channels in mouse sensory neurons. Proc Natl Acad Sci U S A. 2002; 99:2338–2343. [PubMed: 11854527]
8. Askwith CC, Wemmie JA, Price MP, Rokhlina T, Welsh MJ. Acid-sensing ion channel 2 (ASIC2) modulates ASIC1 H+-activated currents in hippocampal neurons. J Biol Chem. 2004; 279:18296–18305. M312145200 [pii]. 10.1074/jbc.M312145200 [PubMed: 14960591]
9. Wemmie JA, et al. The acid-activated ion channel ASIC contributes to synaptic plasticity, learning, and memory. Neuron. 2002; 34:463–477. S089662730200661X [pii]. [PubMed: 11988176]
10. Wemmie JA, et al. Acid-sensing ion channel 1 is localized in brain regions with high synaptic density and contributes to fear conditioning. J Neurosci. 2003; 23:5496–5502. 23/13/5496 [pii]. [PubMed: 12843249]
11. Ziemann AE, et al. The amygdala is a chemosensor that detects carbon dioxide and acidosis to elicit fear behavior. Cell. 2009; 139:1012–1021. [PubMed: 19945383]
12. Wemmie JA, et al. Overexpression of acid-sensing ion channel 1a in transgenic mice increases acquired fear-related behavior. Proc Natl Acad Sci U S A. 2004; 101:3621–3626.10.1073/pnas.0308753101 [PubMed: 14988500]

13. Zha XM, Wemmie JA, Green SH, Welsh MJ. Acid-sensing ion channel 1a is a postsynaptic proton receptor that affects the density of dendritic spines. Proc Natl Acad Sci U S A. 2006; 103:16556–16561. 0608018103 [pii]. 10.1073/pnas.0608018103 [PubMed: 17060608]
14. Zha XM, et al. ASIC2 subunits target acid-sensing ion channels to the synapse via an association with PSD-95. J Neurosci. 2009; 29:8438–8446. 29/26/8438 [pii]. 10.1523/JNEUROSCI.1284-09.2009 [PubMed: 19571134]
15. Baron A, et al. Protein kinase C stimulates the acid-sensing ion channel ASIC2a via the PDZ domain-containing protein PICK1. J Biol Chem. 2002; 277:50463–50468.10.1074/jbc.M208848200 [PubMed: 12399460]
16. Wu PY, et al. Acid-sensing ion channel-1a is not required for normal hippocampal LTP and spatial memory. J Neurosci. 2013; 33:1828–1832. 33/5/1828 [pii]. 10.1523/JNEUROSCI.4132-12.2013 [PubMed: 23365222]
17. Cho JH, Askwith CC. Presynaptic Release Probability Is Increased in Hippocampal Neurons From ASIC1 Knockout Mice. Journal of neurophysiology. 2008; 99:426–441. [PubMed: 18094106]
18. Alvarez de la Rosa D, et al. Distribution, subcellular localization and ontogeny of ASIC1 in the mammalian central nervous system. J Physiol. 2003; 546:77–87. PHY_030692 [pii]. [PubMed: 12509480]
19. Huston JP, Silva MA, Topic B, Muller CP. What's conditioned in conditioned place preference? Trends Pharmacol Sci. 2013; 34:162–166. S0165-6147(13)00005-9 [pii]. 10.1016/j.tips.2013.01.004 [PubMed: 23384389]
20. Napier TC, Herrold AA, de Wit H. Using conditioned place preference to identify relapse prevention medications. Neurosci Biobehav Rev. 2013 S0149-7634(13)00116-4 [pii]. 10.1016/j.neubiorev.2013.05.002
21. White NM, Chai SC, Hamdani S. Learning the morphine conditioned cue preference: cue configuration determines effects of lesions. Pharmacol Biochem Behav. 2005; 81:786–796. S0091-3057(05)00203-0 [pii]. 10.1016/j.pbb.2005.06.002 [PubMed: 16009410]
22. Coryell MW, et al. Restoring Acid-sensing ion channel-1a in the amygdala of knock-out mice rescues fear memory but not unconditioned fear responses. J Neurosci. 2008; 28:13738–13741. 28/51/13738 [pii]. 10.1523/JNEUROSCI.3907-08.2008 [PubMed: 19091964]
23. DeVries SH. Exocytosed protons feedback to suppress the Ca2+ current in mammalian cone photoreceptors. Neuron. 2001; 32:1107–1117. S0896-6273(01)00535-9 [pii]. [PubMed: 11754841]
24. Miesenbock G, De Angelis DA, Rothman JE. Visualizing secretion and synaptic transmission with pH-sensitive green fluorescent proteins. Nature. 1998; 394:192–195. [PubMed: 9671304]
25. Palmer MJ, Hull C, Vigh J, von Gersdorff H. Synaptic cleft acidification and modulation of short-term depression by exocytosed protons in retinal bipolar cells. J Neurosci. 2003; 23:11332–11341. 23/36/11332 [pii]. [PubMed: 14672997]
26. Vessey JP, et al. Proton-mediated feedback inhibition of presynaptic calcium channels at the cone photoreceptor synapse. J Neurosci. 2005; 25:4108–4117. 25/16/4108 [pii]. 10.1523/JNEUROSCI.5253-04.2005 [PubMed: 15843613]
27. Waldmann R, Champigny G, Bassilana F, Heurteaux C, Lazdunski M. A proton-gated cation channel involved in acid-sensing. Nature. 1997; 386:173–177.10.1038/386173a0 [PubMed: 9062189]
28. Krishtal OA, Osipchuk YV, Shelest TN, Smirnoff SV. Rapid extracellular pH transients related to synaptic transmission in rat hippocampal slices. Brain Res. 1987; 436:352–356. [PubMed: 2829992]
29. Gillessen T, Alzheimer C. Amplification of EPSPs by low Ni(2+)- and amiloride-sensitive Ca2+ channels in apical dendrites of rat CA1 pyramidal neurons. Journal of neurophysiology. 1997; 77:1639–1643. [PubMed: 9084628]
30. Manev H, Bertolino M, DeErausquin G. Amiloride blocks glutamate-operated cationic channels and protects neurons in culture from glutamate-induced death. Neuropharmacology. 1990; 29:1103–1110. [PubMed: 1963475]
31. Price MP, et al. The mammalian sodium channel BNC1 is required for normal touch sensation. Nature. 2000; 407:1007–1011. [PubMed: 11069180]

32. Escoubas P, et al. Isolation of a tarantula toxin specific for a class of proton-gated Na+ channels. J Biol Chem. 2000; 275:25116–25121. M003643200 [pii]. 10.1074/jbc.M003643200 [PubMed: 10829030]
33. Sherwood TW, Lee KG, Gormley MG, Askwith CC. Heteromeric acid-sensing ion channels (ASICs) composed of ASIC2b and ASIC1a display novel channel properties and contribute to acidosis-induced neuronal death. J Neurosci. 2011; 31:9723–9734. 31/26/9723 [pii]. 10.1523/JNEUROSCI.1665-11.2011 [PubMed: 21715637]
34. Shah GN, et al. Carbonic anhydrase IV and XIV knockout mice: roles of the respective carbonic anhydrases in buffering the extracellular space in brain. Proc Natl Acad Sci U S A. 2005; 102:16771–16776. 0508449102 [pii]. 10.1073/pnas.0508449102 [PubMed: 16260723]
35. Harris KM, Kater SB. Dendritic spines: cellular specializations imparting both stability and flexibility to synaptic function. Annu Rev Neurosci. 1994; 17:341–371.10.1146/annurev.ne.17.030194.002013 [PubMed: 8210179]
36. Dietz DM, et al. Rac1 is essential in cocaine-induced structural plasticity of nucleus accumbens neurons. Nat Neurosci. 2012; 15:891–896.10.1038/nn.3094 [PubMed: 22522400]
37. Conrad KL, et al. Formation of accumbens GluR2-lacking AMPA receptors mediates incubation of cocaine craving. Nature. 2008; 454:118–121. nature06995 [pii]. 10.1038/nature06995 [PubMed: 18500330]
38. Mameli M, et al. Cocaine-evoked synaptic plasticity: persistence in the VTA triggers adaptations in the NAc. Nat Neurosci. 2009; 12:1036–1041. nn.2367 [pii]. 10.1038/nn.2367 [PubMed: 19597494]
39. Kourrich S, Rothwell PE, Klug JR, Thomas MJ. Cocaine experience controls bidirectional synaptic plasticity in the nucleus accumbens. J Neurosci. 2007; 27:7921–7928. 27/30/7921 [pii]. 10.1523/JNEUROSCI.1859-07.2007 [PubMed: 17652583]
40. Moussawi K, et al. Reversing cocaine-induced synaptic potentiation provides enduring protection from relapse. Proc Natl Acad Sci U S A. 2011; 108:385–390. 1011265108 [pii]. 10.1073/pnas.1011265108 [PubMed: 21173236]
41. Eisch AJ, et al. Brain-derived neurotrophic factor in the ventral midbrain-nucleus accumbens pathway: a role in depression. Biol Psychiatry. 2003; 54:994–1005. [PubMed: 14625141]
42. Shirayama Y, Chen AC, Nakagawa S, Russell DS, Duman RS. Brain-derived neurotrophic factor produces antidepressant effects in behavioral models of depression. J Neurosci. 2002; 22:3251–3261. 20026292. [PubMed: 11943826]
43. Miesenbock G, De Angelis DA, Rothman JE. Visualizing secretion and synaptic transmission with pH-sensitive green fluorescent proteins. Nature. 1998; 394:192–195.10.1038/28190 [PubMed: 9671304]
44. Beg AA, Ernstrom GG, Nix P, Davis MW, Jorgensen EM. Protons act as a transmitter for muscle contraction in C. elegans. Cell. 2008; 132:149–160. S0092-8674(07)01479-1 [pii]. 10.1016/j.cell.2007.10.058 [PubMed: 18191228]
45. Zeng WZ, Xu TL. Proton production, regulation and pathophysiological roles in the mammalian brain. Neurosci Bull. 2012; 28:1–13.10.1007/s12264-012-1068-2 [PubMed: 22233885]
46. Zha XM. Acid-sensing ion channels: trafficking and synaptic function. Mol Brain. 2013; 6:1. 1756-6606-6-1 [pii]. 10.1186/1756-6606-6-1 [PubMed: 23281934]
47. Lee KW, et al. Cocaine-induced dendritic spine formation in D1 and D2 dopamine receptor-containing medium spiny neurons in nucleus accumbens. Proc Natl Acad Sci U S A. 2006; 103:3399–3404. 0511244103 [pii]. 10.1073/pnas.0511244103 [PubMed: 16492766]
48. Golden SA, Russo SJ. Mechanisms of psychostimulant-induced structural plasticity. Cold Spring Harb Perspect Med. 2012; 2 cshperspect.a011957 [pii]. 10.1101/cshperspect.a011957
49. Christoffel DJ, et al. IkappaB kinase regulates social defeat stress-induced synaptic and behavioral plasticity. J Neurosci. 2011; 31:314–321.10.1523/JNEUROSCI.4763-10.2011 [PubMed: 21209217]
50. Jiang Q, Wang CM, Fibuch EE, Wang JQ, Chu XP. Differential regulation of locomotor activity to acute and chronic cocaine administration by acid-sensing ion channel 1a and 2 in adult mice. Neuroscience. 2013; 246:170–178. S0306-4522(13)00392-8 [pii]. 10.1016/j.neuroscience.2013.04.059 [PubMed: 23644053]

51. Radley JJ, Anderson RM, Hamilton BA, Alcock JA, Romig-Martin SA. Chronic stress-induced alterations of dendritic spine subtypes predict functional decrements in an hypothalamo-pituitary-adrenal-inhibitory prefrontal circuit. J Neurosci. 2013; 33:14379–14391.10.1523/jneurosci.0287-13.2013 [PubMed: 24005291]

52. Radley JJ, et al. Repeated stress alters dendritic spine morphology in the rat medial prefrontal cortex. J Comp Neurol. 2008; 507:1141–1150.10.1002/cne.21588 [PubMed: 18157834]

53. Rodriguez A, Ehlenberger DB, Dickstein DL, Hof PR, Wearne SL. Automated three-dimensional detection and shape classification of dendritic spines from fluorescence microscopy images. PLoS One. 2008; 3:e1997.10.1371/journal.pone.0001997 [PubMed: 18431482]

54. LaLumiere RT, Smith KC, Kalivas PW. Neural circuit competition in cocaine-seeking: roles of the infralimbic cortex and nucleus accumbens shell. The European journal of neuroscience. 2012; 35:614–622.10.1111/j.1460-9568.2012.07991.x [PubMed: 22321070]

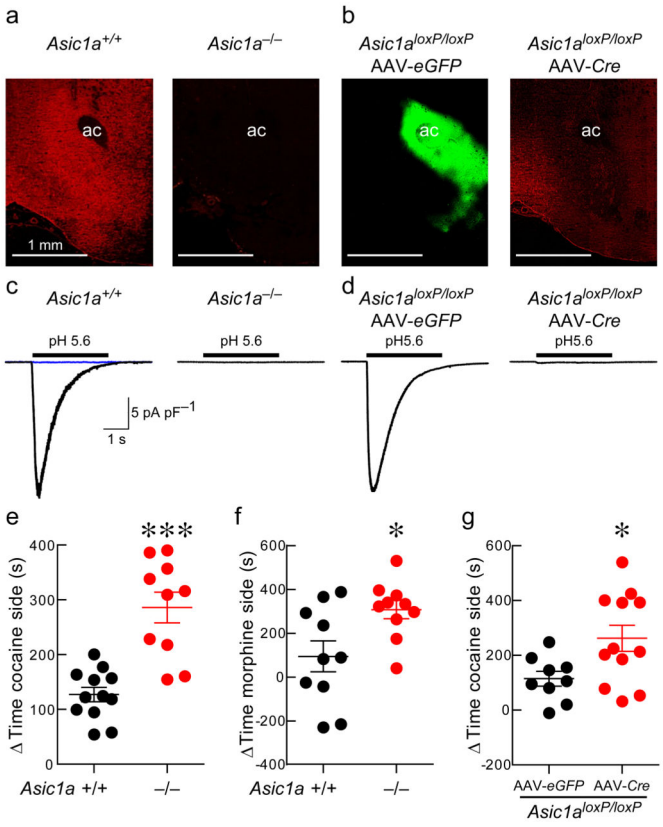

Figure 1. ASIC1A is necessary for acid-evoked currents in the nucleus accumbens (NAc) and disrupting ASIC1A increases conditioned place preference to cocaine and morphine

(a) ASIC1A immunohistochemical labeling in the NAc of *Asic1a*$^{+/+}$ and *Asic1a*$^{-/-}$ mice (ac marks anterior commissure, scale bar indicates 1 mm). (b) Immunohistochemical labeling of *Asic1a*$^{loxP/loxP}$ mouse injected with AAV-*eGFP* and AAV-*Cre* (GFP in green, ASIC1A in red). (c) Representative acid-evoked currents in NAc neurons from *Asic1a*$^{+/+}$ versus *Asic1a*$^{-/-}$ mice. Blue current trace reflects acid-evoked current following amiloride application. (d) Representative acid-evoked currents in NAc neurons from *Asic1a*$^{loxP/loxP}$ mice injected with AAV-*eGFP* or AAV-*Cre*. (e) *Asic1a*$^{-/-}$ mice exhibit a significantly greater cocaine (10 mg/kg) conditioned place preference (CPP) (***$p < 0.001$, Student's *t* test with Welch's correction, n = 10–12). (f) *Asic1a*$^{-/-}$ mice also exhibit greater CPP to morphine (10 mg/kg) (*$p = 0.0184$, Student's *t* test, n = 10). (g) Selective partial knockout of ASIC1A in the nucleus accumbens enhances cocaine (10 mg/kg) CPP (*$p < 0.024$, Student's *t* test, n = 9–12).

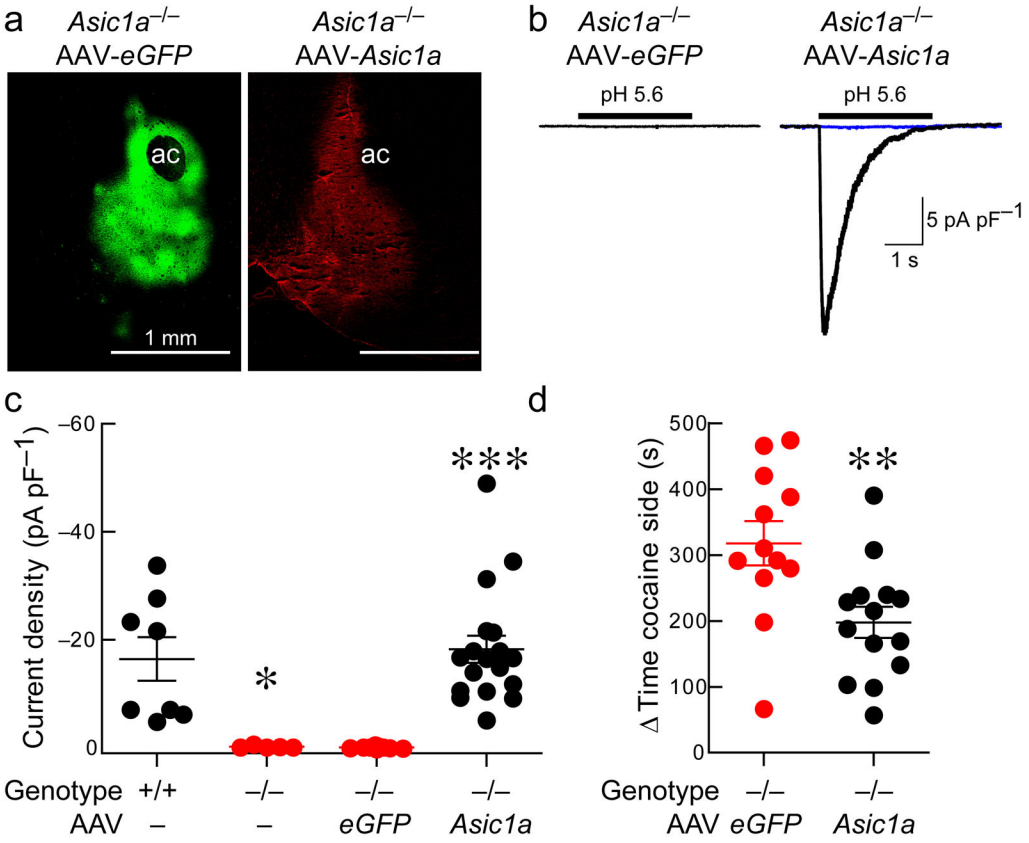

Figure 2. Restoring ASIC1A in the NAc re-establishes acid-evoked currents and reduces cocaine CPP

(a) Immunohistochemical labeling of ASIC1A (in red) and GFP (in green) following NAc injection of AAV-*Asic1a* and AAV-*eGFP* into an *Asic1a*$^{-/-}$ mouse (ac marks anterior commissure, scale bar indicates 1 mm). (b) Representative traces of acid-evoked currents in *Asic1a*$^{-/-}$ mice injected with AAV-*Asic1a* or AAV-*eGFP*. Blue current trace reflects acid-evoked current following amiloride application. (c) Density of pH 5.6-evoked currents in NAc neurons in the indicated groups of mice. Kruskal-Wallis one-way ANOVA revealed significant differences between groups ($H(3) = 29.26$, $p < 0.001$, n = 5–18 neurons). *Asic1a*$^{-/-}$ mice versus *Asic1a*$^{+/+}$ mice (*$p < 0.05$), *Asic1a*$^{-/-}$ mice injected with AAV-*eGFP* versus those injected with AAV-*Asic1a* (***$p < 0.001$, Dunn's Multiple Comparison Test). (d) Restoring ASIC1A expression in the NAc of *Asic1a*$^{-/-}$ mice reduces conditioned place preference to cocaine (10 mg/kg) (**$p = 0.0061$, Student's *t* test, n = 12–14).

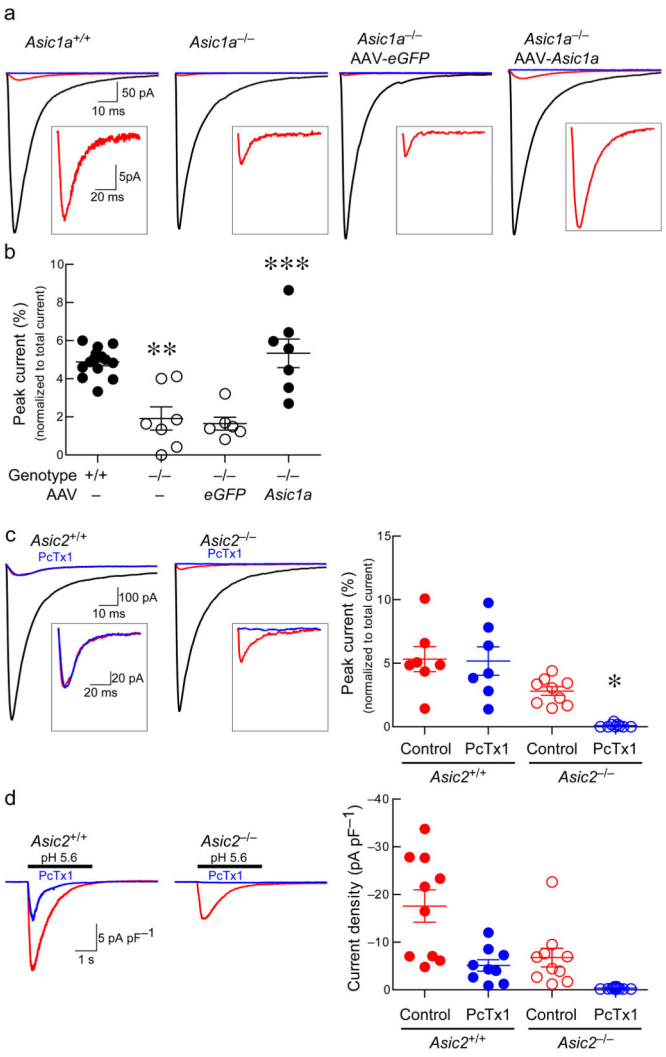

Figure 3. ASIC1A and ASIC2 contribute to synaptic currents in NAc

(a) Representative traces of EPSCs before (black) and after (red) APV, CNQX, picrotoxin, and after APV, CNQX, picrotoxin, amiloride (blue). Inset higher magnification of EPSC sensitive to amiloride but insensitive to APV, CNQX, picrotoxin. (b) Amiloride-sensitive EPSC peak normalized to total EPSC peak. Differences between groups were significant ($F(3, 30) = 17.19$, $p < 0.001$, n = 6–14 neurons, ANOVA). *Asic1a*$^{-/-}$ versus *Asic1a*$^{+/+}$ mice (**$p < 0.01$), AAV-*eGFP* injected *Asic1a*$^{-/-}$ mice versus those injected with AAV-*Asic1a* (***$p < 0.001$, Tukey's). (c) Traces of EPSCs before (black) and after (red) APV, CNQX, picrotoxin, and after APV, CNQX, picrotoxin PcTx1 (blue). Inset illustrates higher magnification of EPSC sensitive to PcTx1 and insensitive to APV, CNQX, and picrotoxin. Bar graph indicates quantification of PcTx1 effects on EPSC peak (insensitive to APV, CNQX, and picrotoxin) normalized to total EPSC peak. A two-way ANOVA revealed a significant effect of genotype ($F(1, 32)$, $p < 0.001$, n = 7–9 neurons), and PcTx1 ($F(1, 32)$, $p < 0.05$, n= 7–9), but no significant interaction ($F(1, 32)$, $p = 0.069$, n = 7–9 neurons). PcTx1 reduced the EPSC in *Asic2*$^{-/-}$ mice (*$p < 0.05$), but not in *Asic2*$^{+/+}$ mice ($p > 0.05$, corrected Bonferroni). (d) Effects of PcTx1 and ASIC2 disruption on pH 5.6-evoked currents (acid-

evoked current in red, current post-PcTx1 in blue). PcTx1 partially inhibited the acid-evoked current in *Asic2*$^{+/+}$ mice and completely inhibited the acid-evoked current in *Asic2*$^{-/-}$ mice. Two-way ANOVA revealed a significant effect of PcTx1 ($F(1, 40)$, $p < 0.001$, $n = 9–11$) and genotype ($F(1, 40)$, $p < 0.001$, $n = 9–11$), but no significant interaction ($F(1, 40)$, $p = 0.147$, $n = 9–11$).

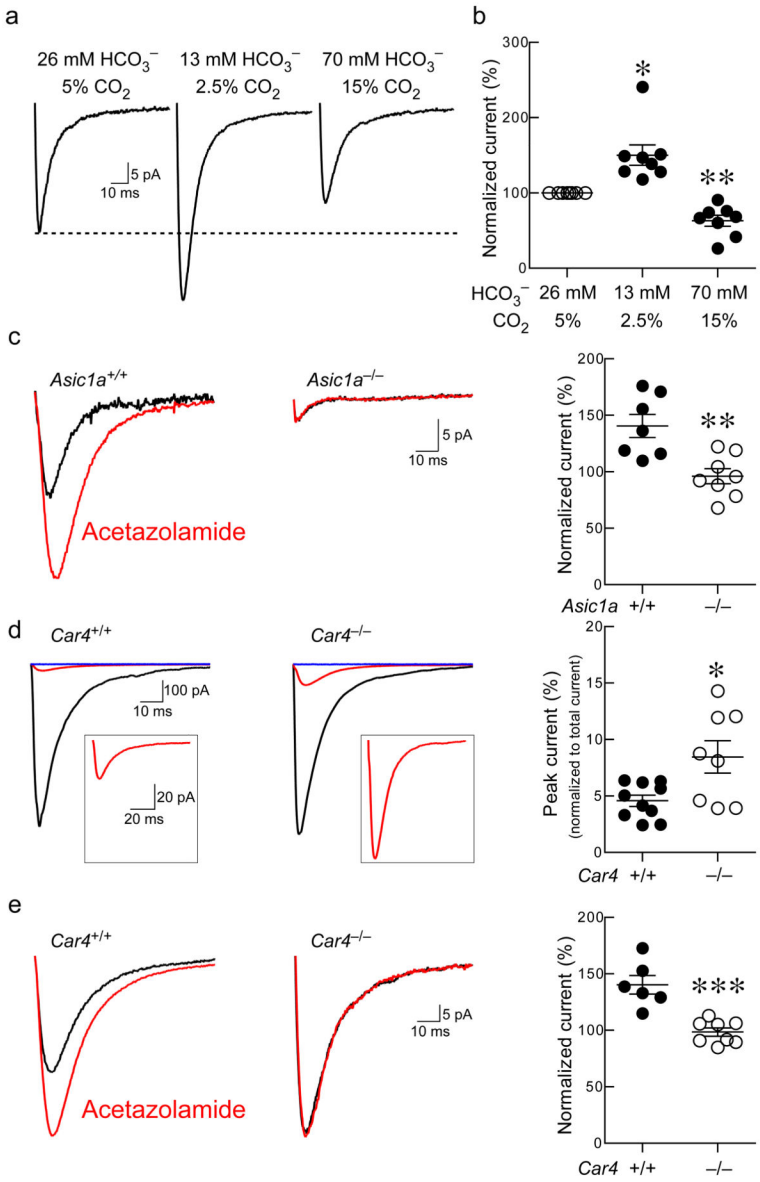

Figure 4. Reducing buffering capacity and inhibiting or deleting carbonic anhydrase IV increased ASIC EPSC in NAc

(a, b) Decreasing the pH- buffering capacity of extracellular solution by reducing HCO_3^- and CO_2 did not alter bath pH (pH 7.3) but increased the ASIC EPSC, whereas increasing the buffering capacity by increasing HCO_3^- and CO_2 produced the opposite effect, normalized to control levels (dashed line). Differences between the groups were significant ($F(2, 23) = 18.83$, $p = 0.0025$, n=8 neurons, repeated-measures ANOVA). Reducing buffering capacity increased ASIC EPSC (*$p < 0.05$), while increasing buffering capacity attenuated ASIC EPSC (**$p < 0.01$, Dunnet's multiple comparisons test). (c) Acetazolamide increased the ASIC EPSC in *Asic1a*$^{+/+}$ mice, but not *Asic1a*$^{-/-}$ mice. Representative traces and quantification of the ASIC-dependent portion of the EPSC (EPSC component insensitive to of APV, CNQX and picrotoxin) with and without acetazolamide in *Asic1a*$^{+/+}$ and *Asic1a*$^{-/-}$ mice (**$p = 0.0025$, Student's *t* test, n = 7–8 neurons). (d) *Car4*$^{-/-}$ mice

exhibited significantly larger ASIC-dependent EPSCs relative to *Car4*$^{+/+}$ mice. Representitive traces of total EPSC (black), ASIC-dependent EPSC (in presence of APV, CNQX and picrotoxin, red), and ASIC-dependent EPSC (with addition of amiloride blue) in the NAc of *Car4*$^{+/+}$ and *Car4*$^{-/-}$ mice. Quantification of ASIC-dependent EPSC peak normalized to total EPSC peak (*$p < 0.013$, Student's *t* test, n = 8–10 neurons). (e) Acetazolamide had no effect on the ASIC-dependent EPSC in *Car4*$^{-/-}$ mice. Representative traces and quantification of the ASIC-dependent EPSC in the presence (red) and absence of acetazolamide (black)(***$p < 0.003$, Student's *t* test, n=6–8 neurons).

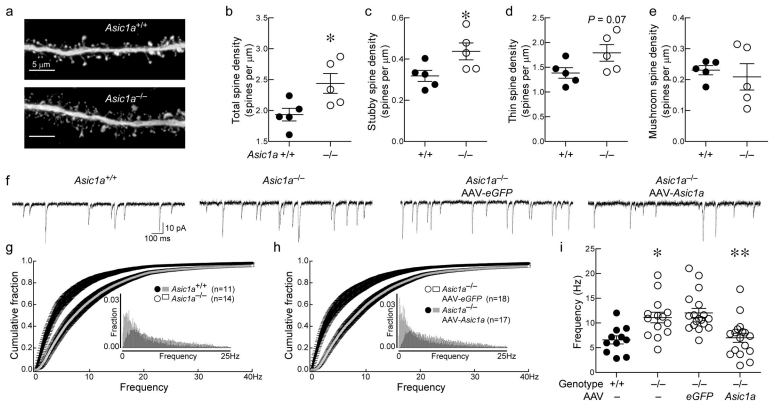

Figure 5. Loss of ASIC1A increases dendritic spine density and mEPSC frequency in the NAc

(a) Representative micrographs of dendritic spines in the NAc of mice of indicated genotypes (scale bar indicates 5 μm). (b, c, d, e) Quantification of spine density in *Asic1a*$^{-/-}$ and *Asic1a*$^{+/+}$ mice: total spines (*p < 0.0295, n=5 mice), stubby spines (*p < 0.0412), thin spines (p = 0.0762), mushroom spines (p = 0.6443). (f) Representive traces of mEPSCs in the NAc of *Asic1a*$^{+/+}$ mice, *Asic1a*$^{-/-}$ mice, and *Asic1a*$^{-/-}$ mice injected with AAV-*Asic1a* or AAV-*eGFP*. (g, h) Cumulative fraction and histograms of mEPSC frequency (insets) from mice of indicated genotypes. (i) mEPSC frequency is significantly elevated in *Asic1a*$^{-/-}$ mice, and restoring ASIC1A in the NAc reduces mEPSC frequency. A one-way ANOVA revealed significant differences between groups ($F(3, 56) = 8.47$, $p<0.001$, n=11–18 neurons per group). *Asic1a*$^{+/+}$ versus *Asic1a*$^{-/-}$ mice (*p < 0.05), *Asic1a*$^{-/-}$ mice injected with AAV-*eGFP* versus those injected with AAV-*Asic1a* (**p < 0.01, Tukey's Multiple Comparison Test).

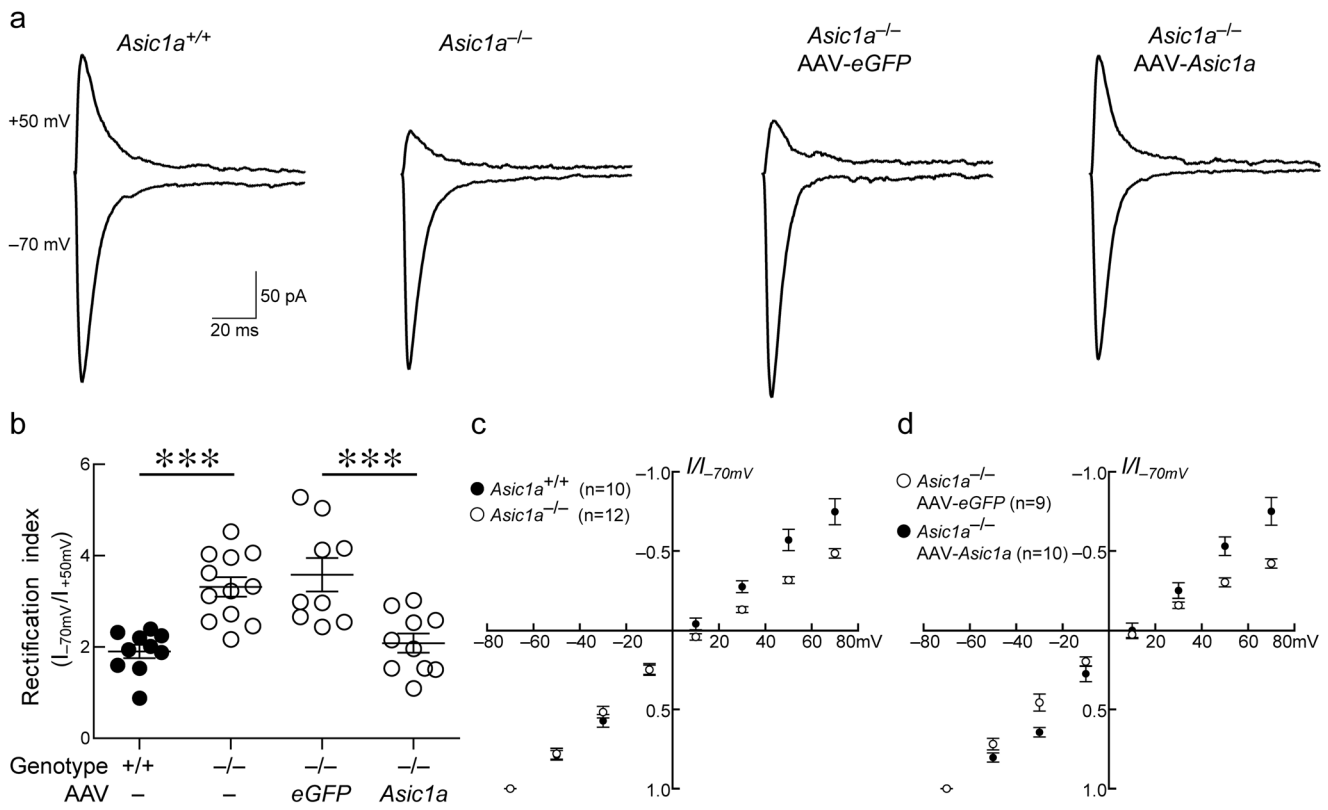

Figure 6. Loss of ASIC1A increases inward rectification of AMPA-mediated EPSCs, which is normalized by re-establishing ASIC1A expression in the NAc

(a) Representative traces of AMPA receptor-mediated current at holding potentials of −70 and +50 mV in NAc neurons of *Asic1a*$^{+/+}$ versus *Asic1a*$^{-/-}$ mice, and *Asic1a*$^{-/-}$ injected with AAV-*Asic1a* versus AAV-*eGFP*. (b) AMPA receptor rectification index is significantly increased in *Asic1a*$^{-/-}$ mice and restoring ASIC1A in the NAc reduces the rectification index to normal levels. One-way ANOVA revealed significant differences between the groups ($F(3, 37) = 12.42$, $p < 0.001$, n=9–12 neurons), *Asic1a*$^{-/-}$ mice versus *Asic1a*$^{+/+}$ mice (***$p < 0.001$) and *Asic1a*$^{-/-}$ mice injected with AAV-*eGFP* versus those injected with AAV-*Asic1a* (***$p < 0.001$, Tukey's Multiple Comparison Test). (c) Current (I/I-70mV) to voltage (mV) relationship for AMPA receptor-mediated currents in *Asic1a*$^{+/+}$ versus *Asic1a*$^{-/-}$ mice, and (d) *Asic1a*$^{-/-}$ mice injected with AAV-*eGFP* versus AAV-*Asic1a*.

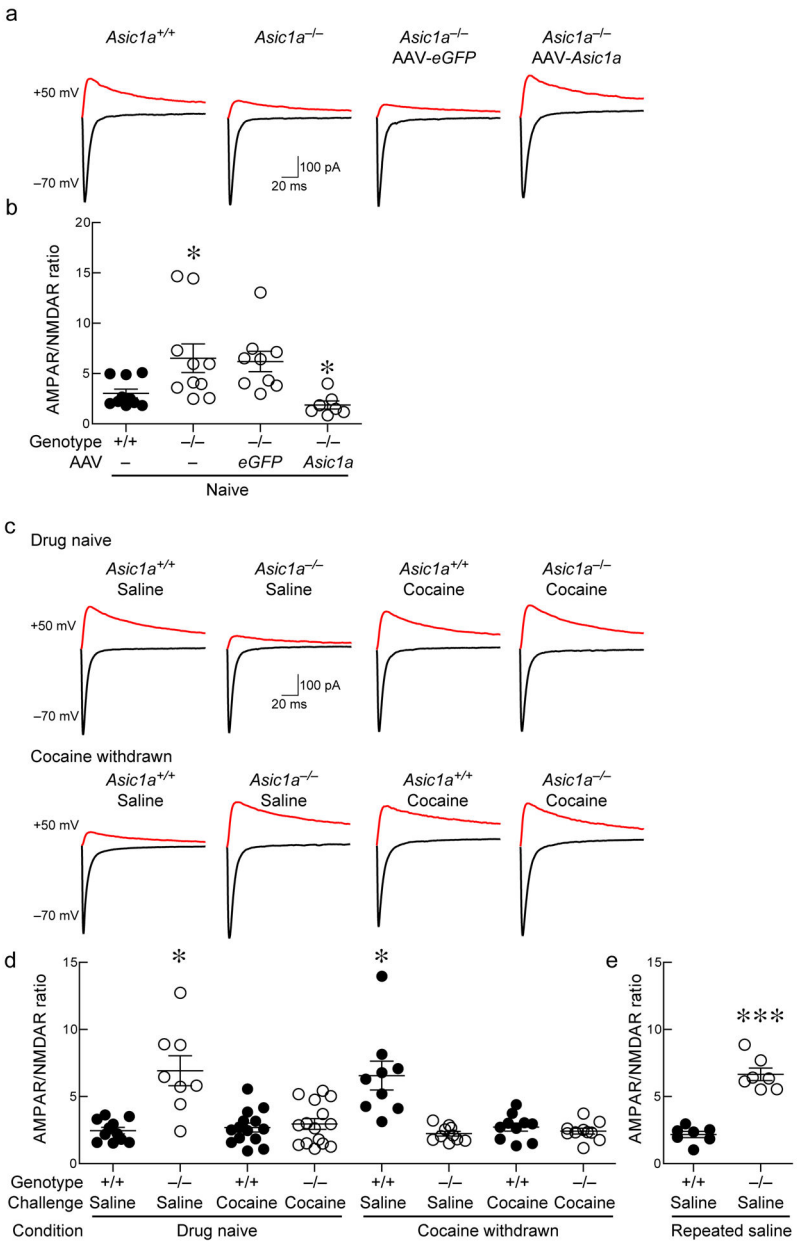

Figure 7. ASIC1A disruption increased AMPA-to-NMDA ratio in NAc, which is acutely reversed by single cocaine dose

(a) Representative traces of AMPA and NMDA receptor-mediated EPSCs in the NAc of indicated mice and *Asic1a*$^{-/-}$ mice injected with AAV-*Asic1a* or AAV-*eGFP*. (b) AMPA-to-NMDA ratios in NAc under indicated conditions. Differences between groups were significant ($F(3, 32) = 5.179$, $p = 0.005$, n=7–10 neurons, ANOVA). AMPA-to-NMDA ratio in *Asic1a*$^{-/-}$ versus to *Asic1a*$^{+/+}$ mice (*$p < 0.05$), *Asic1a*$^{-/-}$ mice injected with AAV-*eGFP* versus those injected with AAV-*Asic1a* (*$p < 0.05$, Sidak's multiple comparisons test). (c) Representative traces of AMPA receptor-mediated and NMDA receptor-mediated EPSCs in the NAc of wild-type and *Asic1a*$^{-/-}$ mice receiving a single dose of saline or cocaine (10 mg/kg, ip), and cocaine withdrawn mice injected with a single challenge dose of saline or

cocaine (10 mg/kg, ip). (d) Quantification of AMPA-to-NMDA ratios in NAc of mice under the indicated conditions. Differences between groups were significant ($H(7) = 32.38$, $p < 0.001$, n = 8–15 neurons, Kruskal-Wallis One-way ANOVA). AMPA-to-NMDA ratio was significantly reduced in naïve *Asic1a*$^{-/-}$ mice injected with a single dose of cocaine compared to saline injected controls (***$p < 0.001$), while a single dose of cocaine did not alter the AMPA-to-NMDA ratio in naïve *Asic1a*$^{+/+}$ mice ($p > 0.05$). A challenge dose of cocaine significantly reduced the AMPA-to-NMDA ratio in cocaine-withdrawn *Asic1a*$^{+/+}$ mice (***$p < 0.001$), but did not alter the AMPA-to-NMDA ratio in cocaine withdrawn *Asic1a*$^{-/-}$ mice ($p > 0.05$, Tukey's). e) *Asic1a*-dependent difference was unaffected by saline injections in separate experiment (***$p < 0.001$, Student's *t* test, n=7 neurons).

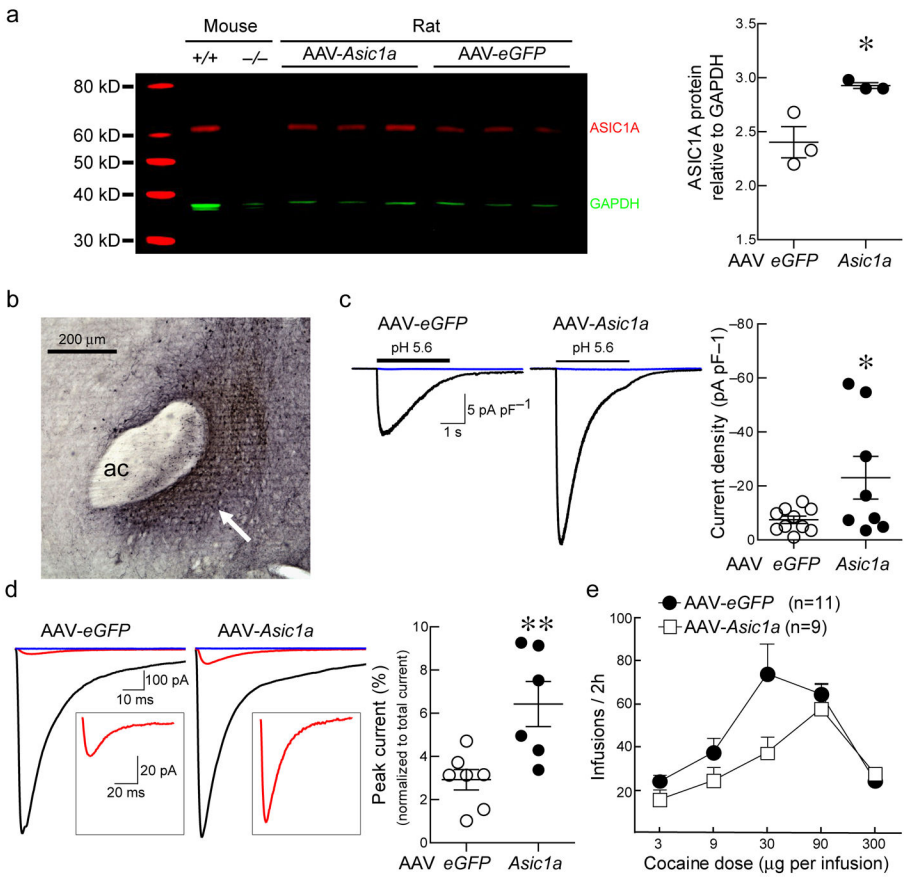

Figure 8. Overexpressing ASIC1A in the rat NAc attenuates cocaine self-administration

(a) Western blot illustrating the effect of AAV-*Asic1a* treatment on rat NAc ASIC1A protein levels. Quantification of the bands shows that AAV-*Asic1a*-treatment significantly increases ASIC1A protein levels in the rat NAc (*p = 0.023, Student's t-test, n = 3 rats). (b) Representative micrograph illustrating GFP immunohistochemistry in the rat NAc, arrow, ac = anterior commissure, scale bar = 200 µm. (c) Representative acid-evoked currents in NAc neurons from AAV-*Asic1a* and AAV-*eGFP* treated rats. Quantification shows a non-significant increase in acid-evoked current density in the AAV-*Asic1a*-treated rats (*p = 0.0456, Student's *t* test, one-tailed, with Welch's correction, n = 8–10 neurons). (d) Representative traces of EPSCs before (black) and after (red) addition of APV, CNQX, and picrotoxin, and after addition of APV, CNQX, picrotoxin and amiloride (blue) in AAV-*Asic1a* and AAV-*eGFP*-transduced rat NAc. Inset illustrates higher magnification of EPSC sensitive to amiloride but insensitive to APV, CNQX, and picrotoxin. Overexpression of ASIC1A in the rat NAc significantly enhanced amiloride-sensitive synaptic currents expressed as % unblocked EPSC peak (**p < 0.0082, Student's t test, n = 6–7 neurons). (e) Rats with AAV-*Asic1a* injected into the NAc showed a rightward shift in cocaine self-administration dose-response and fewer cocaine infusions overall. A two-way repeated-measures ANOVA revealed a significant effect of drug dose ($F(4, 72) = 16.25$, $p < 0.0001$, n = 9–11 rats) and a significant drug dose by AAV-treatment interaction ($F(4, 72) = 2.621$, $p <$

0.0418, n = 9–11 rats). Post-hoc tests revealed that, at the 30 μg dose, rats overexpressing ASIC1A, had significantly fewer infusions than control rats (*$p < 0.05$).